### *In situ* hybridization

See Supplementary Fig. 2.

### Alkaline phosphatase staining

Endogenous alkaline phosphatase activity in 48–72 h.p.f. wholemount zebrafish embryos was detected as described previously[17].

### Deconvolution microscopy

Embryos were fixed overnight at 4 °C in 4% PFA, cryoprotected in 20% sucrose and PBS, snap frozen in 7.5% gelatin and 15% sucrose, and sectioned. Slides were air dried, permeabilized in 1 × PBS, 0.1% Triton X-100 and 1% DMSO, blocked for 20 min in the above solution plus 1% BSA, stained with 66 nM ALEXA Fluor594-phalloidin (Molecular Probes) for 20 min, washed, mounted with Vectashield DAPI (Vector labs), and analysed using a Deltavision Deconvolution Microscope with a × 60 oil objective.

### Immunofluorescent staining

Armenian hamsters were immunized with recombinant murine EGFL7 protein expressed in *Escherichia coli*. Monoclonal antibodies were generated by hybridoma fusion and subcloning. Two monoclonal antibodies, 1C8 and 5H7, that recognize different epitopes were used for immunofluorescent staining. Mouse tissues were snap frozen and cryosectioned. Fixed cells or 5 μm unfixed tissue sections were stained as described[27]. Antibodies used in this study were: anti-ZO-1 monoclonal antibody (catalogue no. 33-9100, Zymed Inc.), anti-GFP (catalogue no. TP401, Torrey Pines Biolabs) and anti-vinculin monoclonal antibody (Sigma).

### Cell-adhesion assay

Plates were coated with 5 μg $cm^{-2}$ protein (BSA (Sigma), collagen (Upstate), fibronectin (Sigma) and recombinant human EGFL7 produced in *E. coli* at Genentech). After PBS rinses, HUVECs (Cambrex) were plated at a density of $5 \times 10^5$ $cm^{-2}$ in EGM2 medium (Cambrex) and centrifuged for 5 min at 140*g* to synchronize cell attachment, and then incubated. To analyse specificity, plates were pre-incubated with the indicated concentrations of antibody before HUVEC plating. Monoclonal anti-human EGFL7 antibody 1B12 was generated at Genentech using the recombinant human EGFL7 protein as immunogen. To determine adhesion strength, inverted plates were centrifuged at 46*g*, 183*g* or 411*g* after 60 min of incubation. The number of adherent cells was quantified using a fluorescence-based assay (CyQUANT, Molecular Probes) and readouts were taken using a fluorescence plate reader (Spectramax, Molecular Devices).

### Accession numbers

GenBank accession numbers for *Egfl7* are as follows: NM_016215 (*Homo sapiens Egfl7*/*VE-statin*), NM_178444 (*Mus musculus Egfl7*), AF184973 (*M. musculus Notch4-like*), P_AAZ37135 (*M. musculus TANGO125*), BC044267 (*Xenopus laevis NEU1*) and AY542170 (*D. rerio Egfl7*). *Egfl8* accession numbers are: NM_030652 (*H. sapiens*) and NM_152922 (*M. musculus*).

Received 4 November 2003; accepted 13 February 2004; doi:10.1038/nature02416.


1. Carmeliet, P. & Jain, R. K. Angiogenesis in cancer and other diseases. *Nature* **407,** 249–257 (2000).
2. Hanahan, D. Signaling vascular morphogenesis and maintenance. *Science* **277,** 48–50 (1997).
3. Hogan, B. L. & Kolodziej, P. A. Organogenesis: molecular mechanisms of tubulogenesis. *Nature Rev. Genet.* **3,** 513–523 (2002).
4. Lubarsky, B. & Krasnow, M. A. Tube morphogenesis: making and shaping biological tubes. *Cell* **112,** 19–28 (2003).
5. Folkman, J. Angiogenesis and angiogenesis inhibition: an overview. *EXS* **79,** 1–8 (1997).
6. Doliana, R., Bot, S., Bonaldo, P. & Colombatti, A. EMI, a novel cysteine-rich domain of EMILINs and other extracellular proteins, interacts with the gC1q domains and participates in multimerization. *FEBS Lett.* **484,** 164–168 (2000).
7. Callebaut, I., Mignotte, V., Souchet, M. & Mornon, J. P. EMI domains are widespread and reveal the probable orthologs of the *Caenorhabditis elegans* CED-1 protein. *Biochem. Biophys. Res. Commun.* **300,** 619–623 (2003).
8. Stainier, D. Y., Weinstein, B. M., Detrich, H. W. III, L. I. & Fishman, M. C. *cloche*, an early acting zebrafish gene, is required by both the endothelial and hematopoietic lineages. *Dev. Suppl.* **121,** 3141–3150 (1995).
9. Soncin, F. *et al.* VE-statin, an endothelial repressor of smooth muscle cell migration. *EMBO J.* **22,** 5700–5711 (2003).
10. Nasevicius, A. & Ekker, S. C. Effective targeted gene 'knockdown' in zebrafish. *Nature Genet.* **26,** 216–220 (2000).
11. Brown, L. A. *et al.* Insights into early vasculogenesis revealed by expression of the ETS-domain transcription factor Fli-1 in wild-type and mutant zebrafish embryos. *Mech. Dev.* **90,** 237–252 (2000).
12. Fouquet, B., Weinstein, B. M., Serluca, F. C. & Fishman, M. C. Vessel patterning in the embryo of the zebrafish: guidance by notochord. *Dev. Biol.* **183,** 37–48 (1997).
13. Liao, W. *et al.* The zebrafish gene *cloche* acts upstream of a *flk-1* homologue to regulate endothelial cell differentiation. *Development* **124,** 381–389 (1997).
14. Lyons, M. S., Bell, B., Stainier, D. & Peters, K. G. Isolation of the zebrafish homologues for the *tie-1* and *tie-2* endothelium-specific receptor tyrosine kinases. *Dev. Dyn.* **212,** 133–140 (1998).
15. Lawson, N. D. & Weinstein, B. M. Arteries and veins: making a difference with zebrafish. *Nature Rev. Genet.* **3,** 674–682 (2002).
16. Zhong, T. P., Rosenberg, M., Mohideen, M.-A. P. n. K., Weinstein, B. & Fishman, M. C. *gridlock*, an HLH gene required for assembly of the aorta in zebrafish. *Science* **287,** 1820–1824 (2000).
17. Childs, S., Chen, J.-N., Garrity, D. M. & Fishman, M. C. Patterning of angiogenesis in the zebrafish embryo. *Development* **129,** 973–982 (2002).
18. Sehnert, A. J. H. A., Weinstein, B. M., Walker, C., Fishman, M. & Stainier, D. Y. Cardiac troponin T is essential in sarcomere assembly and cardiac contractility. *Nature Genet.* **31,** 106–110 (2002).
19. Isogai, S., Lawson, N. D., Torrealday, S., Horiguchi, M. & Weinstein, B. M. Angiogenic network formation in the developing vertebrate trunk. *Development* **130,** 5281–5290 (2003).
20. Sumoy, L., Keasey, J. B., Dittman, T. D. & Kimelman, D. A role for notochord in axial vascular development revealed by analysis of phenotype and the expression of VEGR-2 in zebrafish *flh* and *ntl* mutant embryos. *Mech. Dev.* **63,** 15–27 (1997).
21. Vokes, S. A. & Krieg, P. A. Endoderm is required for vascular endothelial tube formation, but not for angioblast specification. *Dev. Suppl.* **129,** 775–785 (2002).
22. Odenthal, J. & Nusslein-Volhard, C. fork head domain genes in zebrafish. *Dev. Genes Evol.* **208,** 245–258 (1998).
23. Schulte-Merker, S., Ho, R., Herrmann, B. & Nusslein-Volhard, C. The protein product of the zebrafish homologue of the mouse T gene is expressed in nuclei of the germ ring and the notochord of the early embryo. *Development* **116,** 1021–1032 (1992).
24. Strahle, U., Blader, P., Henrique, D. & Ingham, P. Axial, a zebrafish gene expressed along the developing body axis, shows altered expression in cyclops mutant embryos. *Genes Dev.* **7,** 1436–1446 (1993).
25. Parker, L. H., Zon, L. I. & Stainier, D. Y. Vascular and blood gene expression. *Methods Cell Biol.* **59,** 313–336 (1999).
26. Fong, G. H., Zhang, L., Bryce, D. M. & Peng, J. Increased hemangioblast commitment, not vascular disorganization, is the primary defect in *flt-1* knock-out mice. *Development* **126,** 3015–3025 (1999).
27. Ye, W., Shimamura, K., Rubenstein, J. L., Hynes, M. A. & Rosenthal, A. FGF and Shh signals control dopaminergic and serotonergic cell fate in the anterior neural plate. *Cell* **93,** 755–766 (1998).


**Supplementary Information** accompanies the paper on **www.nature.com/nature**.

**Acknowledgements** We thank M. C. Fishman, B. Weinstein and N. Lawson for fish strains, plasmids and helpful discussions; N. Ferrara and H. Gerber for advice and for reviewing the manuscript; J. Lee for the zebrafish cDNA library; L. Rangell for electron microscopy; S. Greenwood for general lab assistance; R. Vandlen, D. Yansura, R. Corpuz and H. Kim for recombinant EGFL7 proteins; A. Chuntharapai and C. Reed for monoclonal antibodies; and W. Wood, H. Clark and J. Tang for bioinformatics assistance. S.J. is supported by the American Heart Association. D.B. is a Human Frontier Science Program Organization fellow.

**Competing interests statement** The authors declare that they have no competing financial interests.

**Correspondence** and requests for materials should be addressed to W.Y. (loni@gene.com).

# Costimulatory signals mediated by the ITAM motif cooperate with RANKL for bone homeostasis

**Takako Koga[1,2]*, Masanori Inui[3]*, Kazuya Inoue[3], Sunhwa Kim[1], Ayako Suematsu[1,2], Eiji Kobayashi[3], Toshio Iwata[3], Hiroshi Ohnishi[4], Takashi Matozaki[4], Tatsuhiko Kodama[5], Tadatsugu Taniguchi[1], Hiroshi Takayanagi[1,2] & Toshiyuki Takai[3]**

[1]*Department of Immunology, Graduate School of Medicine and Faculty of Medicine, University of Tokyo, Hongo 7-3-1, Bunkyo-ku, Tokyo 113-0033, Japan*
[2]*Department of Cellular Physiological Chemistry, Graduate School, Tokyo Medical and Dental University, and COE Program for Frontier Research on Molecular Destruction and Reconstruction of Tooth and Bone, Yushima 1-5-45, Bunkyo-ku, Tokyo 113-8549, Japan and PRESTO, Japan Science and Technology Agency (JST), Honcho 4-1-8, Kawaguchi, Saitama 332-0012, Japan*
[3]*Department of Experimental Immunology, Institute of Development, Aging and Cancer, Tohoku University, Seiryo 4-1, Aoba-ku, Sendai 980-8575, Japan and CREST, JST, Honcho 4-1-8, Kawaguchi, Saitama 332-0012, Japan*
[4]*Biosignal Research Center, Institute for Molecular and Cellular Regulation, Gunma University, Showa-machi 3-39-15, Maebashi 371-8512, Japan*
[5]*Department of Molecular Biology and Medicine, Research Center for Advanced Science and Technology, University of Tokyo, Komaba 4-6-1, Meguro-ku, Tokyo 153-8904, Japan*

* These authors contributed equally to this work

**Costimulatory signals are required for activation of immune cells[1], but it is not known whether they contribute to other biological systems. The development and homeostasis of the skeletal system depend on the balance between bone formation and resorption[2,3]. Receptor activator of NF-κB ligand (RANKL) regulates the differentiation of bone-resorbing cells, osteoclasts, in the presence of macrophage-colony stimulating factor**

**(M-CSF)[4,5]. But it remains unclear how RANKL activates the calcium signals that lead to induction of nuclear factor of activated T cells c1, a key transcription factor for osteoclastogenesis[6]. Here we show that mice lacking immunoreceptor tyrosine-based activation motif (ITAM)[7]-harbouring adaptors[8–10], Fc receptor common γ subunit (FcRγ) and DNAX-activating protein (DAP)12, exhibit severe osteopetrosis owing to impaired osteoclast differentiation. In osteoclast precursor cells, FcRγ and DAP12 associate with multiple immunoreceptors[11–15] and activate calcium signalling through phospholipase Cγ. Thus, ITAM-dependent costimulatory signals activated by multiple immunoreceptors are essential for the maintenance of bone homeostasis. These results reveal that RANKL and M-CSF are not sufficient to activate the signals required for osteoclastogenesis.**

Osteoclast differentiation induced by RANKL and M-CSF is severely blocked in the bone marrow monocyte/macrophage lineage cells (BMMs) derived from mice lacking DAP12 (ref. 16), also known as KARAP or TYROBP[9,10]. DAP12 is a membrane adaptor molecule that contains an ITAM motif, which activates calcium signalling in immune cells. Despite this *in vitro* blockage, DAP12-deficient (*DAP12*$^{-/-}$) mice exhibit only mild osteopetrosis and contain a normal number of osteoclasts. This suggests that the DAP12-mediated signal plays a crucial role in the RANKL/M-CSF-induced osteoclast formation system but that another molecule(s) can rescue the DAP12 deficiency *in vivo*[16].

To investigate the molecular basis of this discrepancy, we stimulated BMMs with RANKL and M-CSF after strictly depleting the stromal/osteoblastic cells[17]. In this osteoblast-free system, osteoclast differentiation is completely abrogated in *DAP12*$^{-/-}$ BMMs (Fig. 1a); we observed no formation of multinucleated cells (MNCs) positive for the marker enzyme of osteoclasts, tartrate-resistant acid phosphatase (TRAP). This differentiation block is efficiently rescued by retroviral expression of DAP12, but not by DAP12Y65F, a DAP12 mutant that does not transmit the ITAM signal[18] (Fig. 1b), indicating that the DAP12-mediated ITAM signal is required for osteoclastogenesis in this system. Interestingly, *DAP12*$^{-/-}$ BMMs undergo osteoclast differentiation in co-culture with osteoblasts[19] (Fig. 1c), showing that osteoblasts can stimulate the signal that compensates for the loss of the DAP12-mediated ITAM signal. This compensatory mechanism may explain the normal osteoclast differentiation in *DAP12*$^{-/-}$ mice *in vivo* (see Supplementary Fig. 1a, b).

The osteoclast-associated receptor (OSCAR) is an activating-type immunoglobulin-like receptor induced in RANKL-stimulated BMMs[11]. Expression of a putative OSCAR ligand in osteoblasts[11] led us to investigate OSCAR as a candidate receptor that compensates for the loss of DAP12-mediated signalling. To explore the adaptor molecules with which OSCAR associates, we constructed a chimaeric receptor composed of the extracellular portion of type IIB FcR for IgG (FcγRIIB) and the transmembrane and cytoplasmic portion of OSCAR (RIIB–OSCAR). Flow-cytometric analysis revealed that RIIB–OSCAR expression was significantly enhanced only when it was cotransfected with FcRγ (Fig. 1d). Thus, RIIB–OSCAR preferentially associates with FcRγ, another adaptor protein containing an ITAM motif, but not with DAP12 or DAP10. Immunoprecipitation analysis also verified the exclusive association of RIIB–OSCAR with FcRγ (Supplementary Fig. 1c).

The results prompted us to investigate the bone phenotype of mice deficient in FcRγ (*FcRγ*$^{-/-}$ mice)[20], but there was no significant difference in the osteoclast number and the trabecular bone volume between wild-type and *FcRγ*$^{-/-}$ mice (Fig. 1e and Supplementary Fig. 1d). In addition, there was little, if any, difference between wild-type and *FcRγ*$^{-/-}$ mice in the differentiation of osteoclasts in the RANKL/M-CSF system (Supplementary Fig. 1e) and the co-culture system (data not shown). Although OSCAR–Fc,

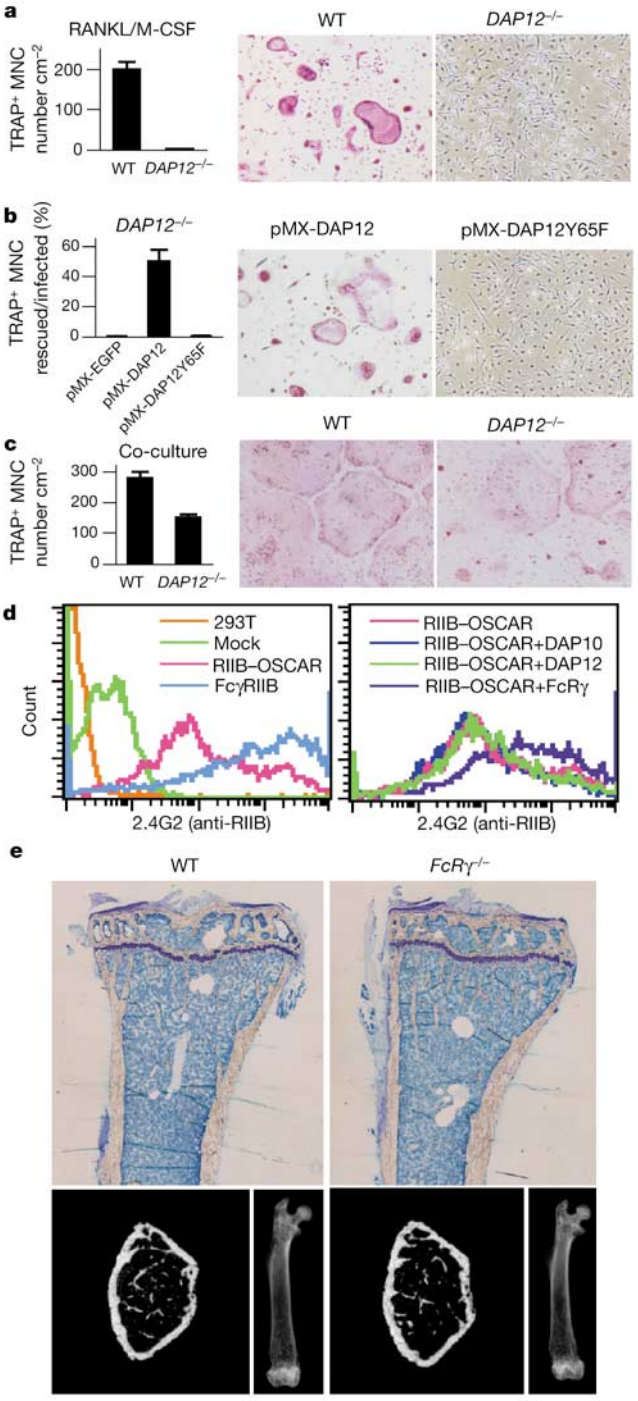


**Figure 1** Impaired osteoclastogenesis in the absence of DAP12 and the compensatory mechanism by osteoblasts. **a**, Complete lack of osteoclastogenesis in *DAP12*$^{-/-}$ BMMs stimulated with RANKL/M-CSF. **b**, Rescue of osteoclastogenesis by retrovirus-mediated expression of DAP12, but not DAP12Y65F, in *DAP12*$^{-/-}$ BMMs. These multinucleated cells have a bone-resorbing activity (not shown). **c**, Osteoclast formation from *DAP12*$^{-/-}$ BMMs in co-culture with osteoblasts. Bone-resorbing activity was examined on dentine slices (not shown). **d**, Flow-cytometric analysis of cell-surface expression of FcγRIIB after overexpression of the chimaeric receptor of RIIB–OSCAR or FcγRIIB (left). Weak expression of FcγRIIB is detected by transfection of RIIB–OSCAR alone (pink line, left and right panels), but cotransfection with FcRγ exclusively increased this expression (violet line, right). **e**, Histology of tibia (upper, toluidine blue staining) and microradiographic analysis of femur (lower, microcomputed tomography, left; microradiograph, right) of *FcRγ*$^{-/-}$ mice. There was no significant abnormality.

a fusion protein of OSCAR ectodomain and Fc portion of IgG, suppresses osteoclastogenesis *in vitro*[11], our results suggest that FcRγ-mediated signals can be compensated for by other signals *in vivo*.

Considering the possibility that DAP12 and FcRγ functionally compensate for each other[21], we generated mice lacking both molecules (*DAP12*$^{-/-}$ *FcRγ*$^{-/-}$ mice). These mice exhibit severe osteopetrosis, with bone marrow filled with unresorbed bone (Fig. 2a). *DAP12*$^{-/-}$ mice show mild osteopetrosis due to impaired osteoclast activity[16], but the osteopetrosis in *DAP12*$^{-/-}$ *FcRγ*$^{-/-}$ mice is much more severe, as seen in microradiographs (Fig. 2a) and trabecular bone volume (Fig. 2b). Importantly, we observed few osteoclasts in *DAP12*$^{-/-}$ *FcRγ*$^{-/-}$ mice, indicating that the osteopetrosis is caused by defective differentiation rather than by defective activity of osteoclasts (Fig. 2c, e). Bone-morphometric analysis revealed that osteoblastic bone formation also decreases (Fig. 2d and Supplementary Fig. 2a). Thus, the ITAM-harbouring adaptors FcRγ and DAP12 are essential for osteoclast differentiation *in vivo*. Despite the severe osteopetrosis in *DAP12*$^{-/-}$ *FcRγ*$^{-/-}$ mice, these mice have no defect in tooth eruption (data not shown). In addition, we observed a very small number of TRAP$^{+}$ MNCs in limited areas just below the epiphyseal plate (Fig. 2e and Supplementary Fig. 2b), suggesting that another adaptor molecule(s) may compensate for the function under specific conditions. In the culture system, *DAP12*$^{-/-}$ *FcRγ*$^{-/-}$ osteoclast precursor cells cannot undergo osteoclast differentiation in response to RANKL and M-CSF (Fig. 3a). Retroviral transfer of *DAP12*, but not *DAP12Y65F* or *FcRγ*, into *DAP12*$^{-/-}$ *FcRγ*$^{-/-}$ cells efficiently rescued osteoclast differentiation induced by RANKL and M-CSF. In addition, *DAP12*$^{-/-}$ *FcRγ*$^{-/-}$ precursor cells barely differentiate into osteoclasts even when co-cultured with osteoblasts (Fig. 3b). In the co-culture system, retroviral transfer of *FcRγ*, but not ITAM-deficient *FcRγY65F*, also rescued osteoclast differentiation, albeit partially. These results suggest that the ITAM signal mediated through FcRγ and DAP12 is indispensable for RANKL-induced osteoclastogenesis and that each adaptor-mediated signal is differentially regulated.

FcRγ or DAP12 associates with several specific immunoreceptors for cell activation in myeloid lineage cells[13,21,22]. To identify receptors that associate with FcRγ and DAP12 in osteoclast lineage cells, we screened the expression profiles of messenger RNAs for known candidate receptors using GeneChip analysis. We found that a series of receptors and ITAM-associated molecules, as well as FcRγ and DAP12, are expressed in the osteoclast lineage (Supplementary Fig. 3a). These putative FcRγ- and DAP12-associating receptors[11–15] were detected on the surface of the osteoclast lineage using cell-surface labelling with biotin (Supplementary Fig. 3b, c). Among these, immunoprecipitation experiments confirmed that paired immunoglobulin-like receptor (PIR)-A, FcγRIII and OSCAR each pair with FcRγ and that triggering receptor expressed by myeloid cells (TREM)-2 and signal-regulatory protein (SIRP)β1, but not NKG2D, pair with DAP12 in the osteoclast lineage (Fig. 3c).

To test whether these receptor-mediated signals promote osteoclast differentiation by associating with FcRγ or DAP12, we stimulated BMMs with plate-bound monoclonal antibodies against OSCAR, PIR, TREM-2 and SIRPβ1. Triggering of either receptor by crosslinking with an antibody accelerated RANKL-induced osteoclast differentiation, indicating that these receptors activate osteoclastogenesis, although the stimulatory effect is more obvious at a low concentration of RANKL (Fig. 3d and Supplementary Fig. 3d). In the absence of RANKL, the stimulation of these receptors alone could not induce osteoclast differentiation (data not shown), suggesting that these receptor-mediated signals act cooperatively with RANKL but cannot substitute for the signal.

A stimulating effect by anti-OSCAR and anti-PIR antibodies was not observed in *FcRγ*$^{-/-}$ BMMs, whereas anti-TREM-2 and anti-

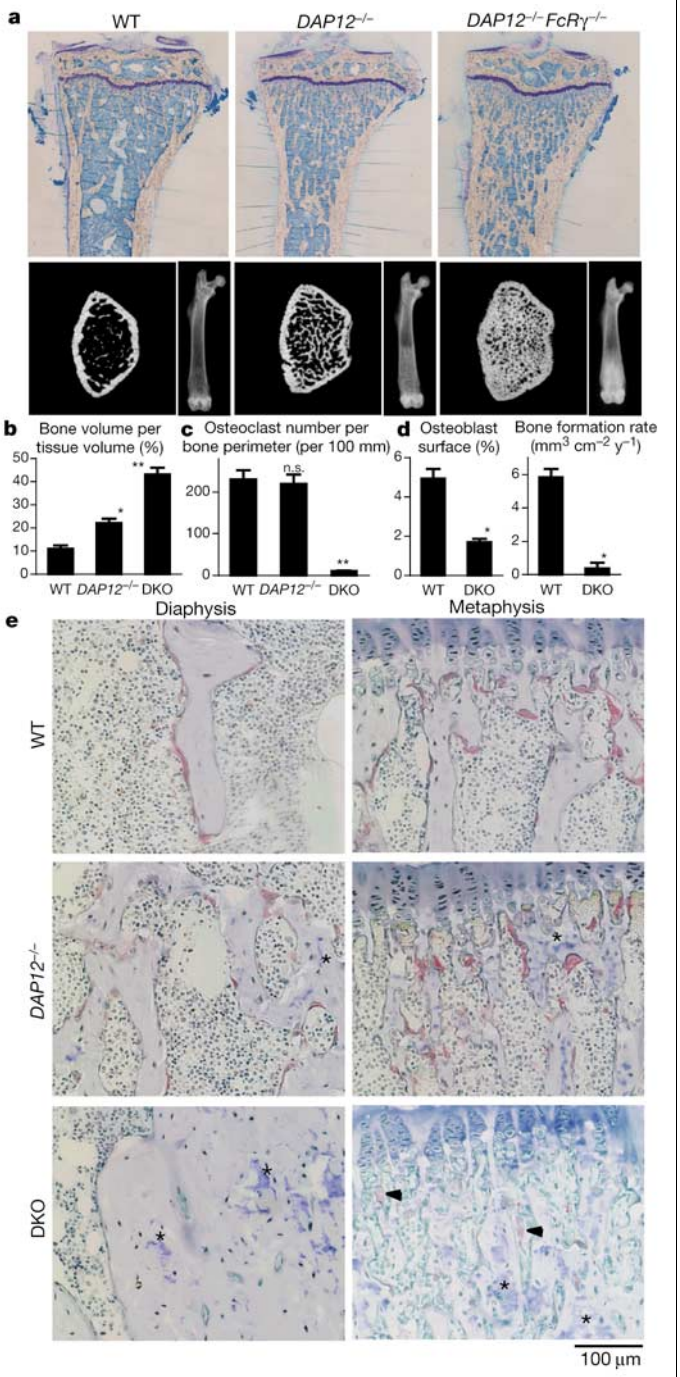


**Figure 2** Severe osteopetrosis in *DAP12*$^{-/-}$ *FcRγ*$^{-/-}$ (DKO) mice due to impaired osteoclast differentiation. **a**, Histology of tibia and microradiographic analysis of femur of *DAP12*$^{-/-}$ and *DAP12*$^{-/-}$ *FcRγ*$^{-/-}$ mice (12 weeks of age). Bone-marrow cavity is absent in *DAP12*$^{-/-}$ *FcRγ*$^{-/-}$ mice. Higher radiopacity shows that *DAP12*$^{-/-}$ *FcRγ*$^{-/-}$ mice have a much more severe osteopetrotic phenotype than *DAP12*$^{-/-}$ mice. **b**, Increased trabecular bone volume in *DAP12*$^{-/-}$ *FcRγ*$^{-/-}$ mice. **c**, The number of osteoclasts is not altered in *DAP12*$^{-/-}$ mice, but is markedly decreased in *DAP12*$^{-/-}$ *FcRγ*$^{-/-}$ mice. **d**, Osteoblastic parameters in the bone-morphometric analysis of the tibia of wild-type and *DAP12*$^{-/-}$ *FcRγ*$^{-/-}$ mice (12 weeks of age). **e**, Histology of the tibia of *DAP12*$^{-/-}$ and *DAP12*$^{-/-}$ *FcRγ*$^{-/-}$ mice (TRAP and toluidine blue staining). Bone-marrow cavity is filled with unresorbed bone in the diaphysis of *DAP12*$^{-/-}$ *FcRγ*$^{-/-}$ mice. No osteoclasts are observed in the diaphysis of *DAP12*$^{-/-}$ *FcRγ*$^{-/-}$ mice, whereas the osteoclast number is normal in *DAP12*$^{-/-}$ mice. Typical sites of cartilage remnant are indicated by asterisks. In the metaphyseal area, a small number of osteoclasts are observed below epiphyseal plates in *DAP12*$^{-/-}$ *FcRγ*$^{-/-}$ mice (arrowheads).

SIRPβ1 antibodies stimulated *FcRγ*$^{-/-}$ BMMs, the same as they did with wild-type cells (Fig. 3e). This indicates that FcRγ is required for the stimulatory function of OSCAR and PIR-A. Consistent with the observation that osteoblasts rescue DAP12 deficiency through FcRγ-associated receptors, anti-OSCAR and anti-PIR antibodies could rescue the osteoclastogenesis from *DAP12*$^{-/-}$ BMMs but not from *DAP12*$^{-/-}$ *FcRγ*$^{-/-}$ cells (Fig. 3f). Stimulation of DAP12-associating receptors such as TREM-2 and SIRPβ1 did not rescue *DAP12*$^{-/-}$ BMMs. This indicates that DAP12 is required for the stimulatory effect through TREM-2 and SIRPβ1 (Fig. 3f).

How does the ITAM signal contribute to RANKL-induced signalling events? To address this question, we performed a genome-wide screening of mRNA expression in RANKL-stimulated osteoclast precursor cells derived from wild-type and *DAP12*$^{-/-}$ *FcRγ*$^{-/-}$ mice. Among the transcription factors and effector molecules involved in RANKL signalling[6], the induction of nuclear factor of activated T cells c1 (NFATc1) is most strongly suppressed in *DAP12*$^{-/-}$ *FcRγ*$^{-/-}$ cells (Fig. 4a). We analysed the protein expression of essential molecules for osteoclastogenesis[2,4,6] including NFATc1, c-Fos and TRAF6, and revealed that NFATc1 expression in *DAP12*$^{-/-}$ *FcRγ*$^{-/-}$ cells stimulated with RANKL is barely detectable, but the expression of c-Fos or TRAF6 is still observed under the same conditions (Supplementary Fig. 4a). To confirm the crucial role of NFATc1 as a downstream target, we examined whether ectopic expression of NFATc1, c-Fos or TRAF6 by retrovirus-mediated gene transfer rescues the differentiation block of osteoclasts in *DAP12*$^{-/-}$ *FcRγ*$^{-/-}$ cells. Ectopic expression of NFATc1, but not c-Fos or TRAF6, resulted in efficient osteoclast formation even in *DAP12*$^{-/-}$ *FcRγ*$^{-/-}$ cells (Fig. 4b).

RANKL-induced calcium signalling is essential for autoamplification of the *NFATc1* gene during osteoclastogenesis[6], whereas immunoglobulin-like receptors activate phospholipase Cγ (PLCγ) and calcium signalling through ITAM in immune cells[13,21]. We therefore examined calcium signalling in RANKL-stimulated osteoclast precursor cells derived from *DAP12*$^{-/-}$ *FcRγ*$^{-/-}$ mice. As shown in Fig. 4c, calcium oscillation induced by RANKL is not significantly observed in *DAP12*$^{-/-}$ *FcRγ*$^{-/-}$ cells, which suggests that the inhibition of this calcium signalling explains the impaired induction of NFATc1. Furthermore, stimulation with the anti-PIR antibody rescued the defect in calcium signalling and NFATc1 expression in *DAP12*$^{-/-}$ cells, suggesting that the stimulation of an immunoreceptor is required for RANKL-induced activation of the calcium signal leading to NFATc1 induction and osteoclastogenesis (Fig. 4c and Supplementary Fig. 4b). These findings suggest that FcRγ and DAP12 are required for the induction of NFATc1, the crucial step in the RANKL-induced osteoclast

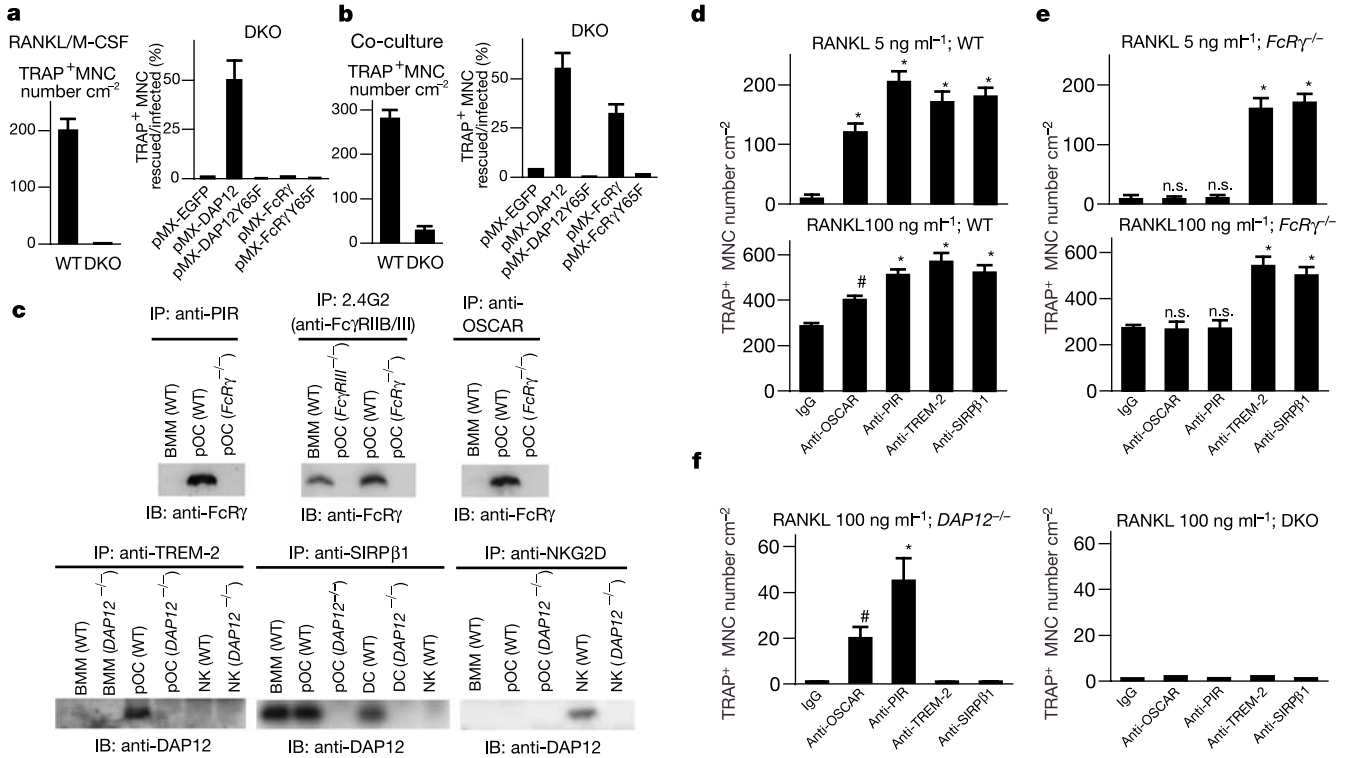


**Figure 3** Distinct roles of FcRγ- and DAP12-associating immunoreceptors in the regulation of osteoclastogenesis. **a**, Complete block of *in vitro* osteoclastogenesis in *DAP12*$^{-/-}$ *FcRγ*$^{-/-}$ (DKO) cells stimulated with RANKL and M-CSF. This was rescued by pMX-DAP12, but not pMX-DAP12Y65F or pMX-FcRγ. **b**, Severe impairment of osteoclastogenesis in *DAP12*$^{-/-}$ *FcRγ*$^{-/-}$ cells even in co-culture with osteoblasts. Osteoclastogenesis was rescued by pMX-DAP12 or pMX- FcRγ in an ITAM-dependent manner. **c**, Association of FcRγ with PIR-A, FcγRIII and OSCAR (upper). pOC, osteoclast precursor cells stimulated with RANKL. For the comments on the association of FcRγ with FcγRIII, see Supplementary Fig. 3b, c. Association of DAP12 with TREM-2 and SIRPβ1, but not with NKG2D, in pOC (lower). For the positive control, DAP12 associates with SIRPβ1 and NKG2D in dendritic cells (DC) and NK cells (NK), respectively. **d**, Treatment of BMMs with plate-bound monoclonal antibodies against OSCAR, PIR, TREM-2 or SIRPβ1 promotes osteoclastogenesis stimulated by RANKL and M-CSF. The stimulatory effect by antibody-mediated crosslinking is more obvious at a low concentration of RANKL (5 ng ml$^{-1}$) than at a high concentration (100 ng ml$^{-1}$). **e**, Effect of plate-bound antibodies on osteoclastogenesis from *FcRγ*$^{-/-}$ BMMs. Anti-OSCAR and anti-PIR antibodies have no effect on *FcRγ*$^{-/-}$ BMMs. **f**, Effect of plate-bound antibodies on osteoclastogenesis from *DAP12*$^{-/-}$ BMMs or *DAP12*$^{-/-}$ *FcRγ*$^{-/-}$ cells stimulated with RANKL/M-CSF. Anti-OSCAR and anti-PIR antibodies rescued osteoclastogenesis from *DAP12*$^{-/-}$BMMs, but such an effect was not observed in anti-TREM-2 or anti-SIRPβ1 antibodies. No stimulatory effect was observed on osteoclastogenesis from *DAP12*$^{-/-}$ *FcRγ*$^{-/-}$ cells.

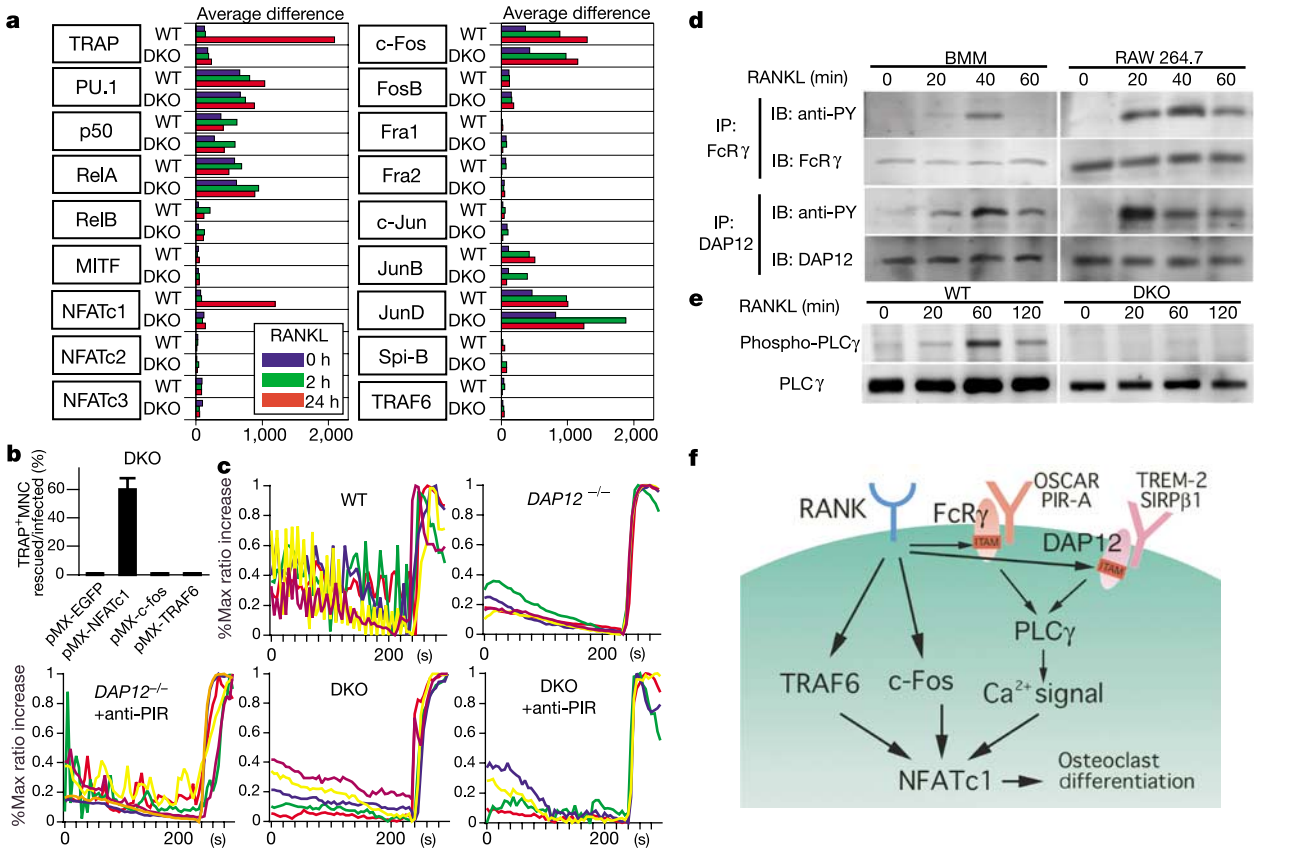


**Figure 4** ITAM-harbouring adaptors are essential for RANKL induction of calcium signalling and NFATc1. **a**, GeneChip analysis of mRNA expression of transcription factors and effector molecules involved in RANKL signalling. NFATc1 induction is most strongly impaired in *DAP12*$^{-/-}$ *FcRγ*$^{-/-}$ (DKO) cells. **b**, Introduction of NFATc1 by pMX retrovirus vector (pMX-NFATc1) into the *DAP12*$^{-/-}$ *FcRγ*$^{-/-}$ precursor cells efficiently rescued the osteoclastogenesis (with bone-resorbing activity; not shown) in the presence of RANKL and M-CSF. **c**, Calcium signalling in osteoclast precursor cells stimulated with RANKL and M-CSF for 24 h. Calcium oscillation was not observed in *DAP12*$^{-/-}$ *FcRγ*$^{-/-}$ or *DAP12*$^{-/-}$ cells. Stimulation with plate-bound anti-PIR antibody rescued the calcium signalling in *DAP12*$^{-/-}$ cells, but not in *DAP12*$^{-/-}$ *FcRγ*$^{-/-}$ cells. **d**, Phosphorylation of FcRγ and DAP12 by RANKL. Phosphorylation of FcRγ and DAP12 induced by RANKL in BMMs as well as in RAW 264.7 cells. PY, phosphotyrosine. **e**, Impaired phosphorylation of PLCγ1 by RANKL in *DAP12*$^{-/-}$ *FcRγ*$^{-/-}$ cells. **f**, A schematic model of ITAM-mediated costimulatory signal in RANKL-stimulated induction of osteoclast differentiation. Phosphorylation of ITAM stimulated by immunoreceptors and RANKL–RANK interaction results in the recruitment of Syk family kinases, leading to the activation of PLCγ and calcium signalling, which is critical for NFATc1 induction. NFATc1 induction is also dependent on c-Fos and TRAF6, both of which are activated by RANKL. RANKL may also contribute to efficient ITAM signalling through the induction of immunoreceptors or their putative ligands.

differentiation programme, through activation of calcium signalling.

To gain further insight into the mechanism linking RANKL and ITAM-mediated calcium signalling, we analysed the phosphorylation events induced by RANKL. Our analysis revealed that RANKL induces the phosphorylation of both FcRγ and DAP12 in BMMs as well as in RAW 264.7 cells (Fig. 4d). We further demonstrated that RANKL-induced phosphorylation of PLCγ is impaired in *DAP12*$^{-/-}$ *FcRγ*$^{-/-}$ cells (Fig. 4e), but RANKL-induced phosphorylation of p38, JNK and IκB is not affected (Supplementary Fig. 4c). This suggests that FcRγ and DAP12 are specifically involved in the PLCγ–calcium pathway. In addition, piceatannol, the inhibitor of Syk kinase, which is recruited to ITAM in immune cells, has an inhibitory effect on osteoclastogenesis (Supplementary Fig. 4d).

Our results show that the ITAM-harbouring adaptors FcRγ and DAP12 deliver essential signals, in concert with RANK-induced signalling cascades, for terminal differentiation of osteoclasts. Our study establishes the importance of the ITAM-mediated costimulatory signal in RANKL-induced osteoclast differentiation (Fig. 4f), which is analogous to the role of costimulatory signals in the immune system[13,21]. Although most of the ligands for the immunoreceptors remain to be identified, putative ligands are provided by distinct cell types: osteoclast precursor cells themselves stimulate exclusively DAP12-associated receptors, but osteoblasts also stimulate FcRγ-associated receptors. The defective osteoblast function in *DAP12*$^{-/-}$ *FcRγ*$^{-/-}$ mice suggests that the osteoclast–osteoblast communication through these receptors may couple bone resorption to formation. It remains to be elucidated whether inhibitory receptors such as FcγRIIB and PIR-B (Supplementary Fig. 3a) contribute to counterbalancing the ITAM signal in osteoclast differentiation. It is notable that osteoclastogenesis is enhanced in mice lacking phosphatases such as SHP-1 or SHIP-1, which counterbalance the ITAM signal in the immune system[23,24]. The mutations of the ITAM-harbouring adaptors and their associating receptors are related to pathological conditions in the skeletal system[25–27], suggesting that the regulation of costimulatory signals may provide a novel strategy for the treatment of skeletal disorders. □

## Methods

### Mice and analysis of bone phenotype

*DAP12*$^{-/-}$ *FcRγ*$^{-/-}$ mice were generated by crossing between *DAP12*$^{+/-}$ *FcRγ*$^{+/-}$ males and females obtained by mating of *DAP12*$^{-/-}$ mice in the 129/SvJ and C57BL/6 (B6)

hybrid background[16] with *FcRγ*$^{-/-}$ mice in B6 background[20]. *DAP12*$^{-/-}$ *FcRγ*$^{-/-}$ mice grow normally and are fertile, without gross abnormalities. *FcγRIII*$^{-/-}$ mice have been described previously[28]. All experiments were performed with appropriate littermate controls. Histological, histomorphometric and microradiographic examinations were performed using essentially the same method as described previously[29]. Statistical analysis was performed using the Student's *t*-test (#$P < 0.05$, *$P < 0.01$, **$P < 0.001$). All mice were born and kept under pathogen-free conditions.

### Flow cytometry and immunoprecipitation

Complementary DNAs for *FcRγ*, *DAP12*, *DAP10* and *RIIB–OSCAR* chimaera coding for the extracellular domain of FcγRIIB and the transmembrane and cytoplasmic portion of OSCAR were inserted into the pIRES-puro vector (BD Biosciences). 293T cells were transfected transiently with these vectors, harvested after 48 h, stained with PE-conjugated anti-FcγRIIB/III antibody (2.4G2) and monitored by flow cytometry. For immunoprecipitation, cells were lysed with digitonin buffer (1% digitonin, 13.6 mM triethanolamine, 150 mM NaCl, 1 mM EDTA, 10 mM iodoacetamide, protease inhibitors, pH 7.8). Cell lysates were incubated with 2.4G2 (ATCC), anti-OSCAR, anti-TREM-2 (6E9) (prepared by T. Takai), anti-PIR (6C1, a gift from H. Kubagawa), anti-NKG2D (Santa Cruz) and anti-SIRPβ1 (prepared by T. M.) antibodies and Protein A Sepharose. The specificity of newly prepared antibodies was determined using flow cytometry, and their agonistic effects on ITAM-mediated signalling events were confirmed. Immunoprecipitates were separated by SDS-polyacrylamide gel electrophoresis (PAGE) and immunoblotted with anti-FcRγ or -DAP12 antibodies (prepared by T. Takai).

### *In vitro* osteoclastogenesis

We have described our method of *in vitro* osteoclastogenesis previously[17,29]. Briefly, after depleting adherent cells, non-adherent bone marrow cells were cultured in α-MEM (Gibco BRL) with 10% FBS (Sigma) containing 10 ng ml$^{-1}$ M-CSF (Genzyme). After two days, adherent cells were used as BMMs. Monocyte/macrophage progenitor cells of *DAP12*$^{-/-}$ *FcRγ*$^{-/-}$ mice were derived from the spleen and similarly cultured with M-CSF for 2 days. These osteoclast precursor cells were further cultured in the presence of 100 ng ml$^{-1}$ soluble RANKL (Peprotech) and 10 ng ml$^{-1}$ M-CSF to generate osteoclasts (RANKL/M-CSF system). RANKL/M-CSF were used at these concentrations throughout the paper unless otherwise described. To examine the *in vitro* osteoclastogenesis from *DAP12*$^{-/-}$ BMMs, the contamination of stromal/osteoblastic cells should be strictly avoided[17]. These culture conditions are different from those previously described[16], in which osteoclast formation was not completely blocked. The co-culture of osteoclast precursor cells and osteoblasts derived from calvarial cells was performed in the presence of $10^{-8}$ M 1, 25 $(OH)_2$ vitamin $D_3$ and $10^{-6}$ M dexamethasone in the absence of recombinant RANKL and M-CSF as described previously[19]. Three to five days later, TRAP$^+$ multinucleated (more than three nuclei) cells were counted. All data are expressed as mean ± s.e.m. ($n = 6$). TRAP$^+$ MNCs were characterized by examining the bone-resorbing activity on dentine slices as described previously[6]. For crosslinking experiments, culture plates were preincubated with PBS containing 5 μg ml$^{-1}$ antibody at 4 °C for 24 h before seeding precursor cells.

### Retroviral gene transduction

Retroviral vectors pMX-DAP12, pMX-DAP12Y65F, pMX-FcRγ and pMX- FcRγY65F were constructed by inserting *DAP12* or *FcRγ* cDNA, and their mutant cDNAs generated by PCR-directed mutagenesis into pMX-IRES-EGFP vector[17]. Other vectors such as pMX-NFATc1, pMX-c-fos and pMX-TRAF6 have been described previously, and packaging was performed as described elsewhere[6,29]. Two days after inoculation, BMMs were cultured with RANKL and M-CSF. After four days, osteoclastogenesis was evaluated by TRAP staining. The rescuing effect was normalized by measuring infection efficiency assessed by GFP expression as previously described[6,29].

### GeneChip analysis

RNA extraction was previously described[6]. Total RNA (15 μg) was used for cDNA synthesis by reverse transcription followed by synthesis of biotinated cRNA through *in vitro* transcription. After cRNA fragmentation, hybridization with mouse U74Av2 or A430 GeneChip (Affymetrix) was performed and analysed according to the manufacturer's protocol. GeneChip analysis was repeated several times and yielded similar results; a representative set of data is shown.

### Calcium measurement

Osteoclast precursor cells were incubated with RANKL in the presence of M-CSF for 24 h and subjected to calcium measurement as previously described[6]. RANKL does not induce a calcium spike immediately in the osteoclast precursor cells, although it does so in the mature osteoclasts[6,30].

### Phosphorylation of FcRγ/DAP12 and PLCγ

Osteoclast precursor cells or RAW 264.7 cells were stimulated by 100 ng ml$^{-1}$ soluble RANKL after 6 h of serum starvation. After various time periods, cell extracts were harvested from the cells using TNE buffer containing 10 mM Tris-HCl (pH 7.8), 150 mM NaCl, 1 mM EDTA, 1% NP-40, 2 mM $Na_3VO_4$, 10 mM NaF and 10 μg ml$^{-1}$ aprotinin. Cell extracts were incubated with 1 μg of anti-DAP12 or anti-FcRγ antibodies for 1 h at 4 °C. Immune complexes were recovered with Protein A Sepharose, subjected to SDS-PAGE and blotted with anti-phosphotyrosine antibody (4G10, Upstate) or the indicated antibodies. Activation of PLCγ was detected using anti-PLCγ1 and anti-phospho-PLCγ1 antibodies (Santa Cruz).

Received 2 December 2003; accepted 23 February 2004; doi:10.1038/nature02444.


1. Lenschow, D. J., Walunas, T. L. & Bluestone, J. A. CD28/B7 system of T cell costimulation. *Annu. Rev. Immunol.* **14,** 233–258 (1996).
2. Karsenty, G. & Wagner, E. F. Reaching a genetic and molecular understanding of skeletal development. *Dev. Cell.* **2,** 389–406 (2002).
3. Rodan, G. A. & Martin, T. J. Therapeutic approaches to bone diseases. *Science* **289,** 1508–1514 (2000).
4. Teitelbaum, S. L. & Ross, F. P. Genetic regulation of osteoclast development and function. *Nature Rev. Genet.* **4,** 638–649 (2003).
5. Boyle, W. J., Simonet, W. S. & Lacey, D. L. Osteoclast differentiation and activation. *Nature* **423,** 337–342 (2003).
6. Takayanagi, H. *et al.* Induction and activation of the transcription factor NFATc1 (NFAT2) integrate RANKL signaling in terminal differentiation of osteoclasts. *Dev. Cell.* **3,** 889–901 (2002).
7. Reth, M. Antigen receptor tail clue. *Nature* **338,** 383–384 (1989).
8. Perez-Montfort, R., Kinet, J. P. & Metzger, H. A previously unrecognized subunit of the receptor for immunoglobulin E. *Biochemistry* **22,** 5722–5728 (1983).
9. Olcese, L. *et al.* Human killer cell activatory receptors for MHC class I molecules are included in a multimeric complex expressed by natural killer cells. *J. Immunol.* **158,** 5083–5086 (1997).
10. Lanier, L. L., Corliss, B. C., Wu, J., Leong, C. & Phillips, J. H. Immunoreceptor DAP12 bearing a tyrosine-based activation motif is involved in activating NK cells. *Nature* **391,** 703–707 (1998).
11. Kim, N., Takami, M., Rho, J., Josien, R. & Choi, Y. A novel member of the leukocyte receptor complex regulates osteoclast differentiation. *J. Exp. Med.* **195,** 201–209 (2002).
12. Kubagawa, H., Burrows, P. D. & Cooper, M. D. A novel pair of immunoglobulin-like receptors expressed by B cells and myeloid cells. *Proc. Natl Acad. Sci. USA* **94,** 5261–5266 (1997).
13. Colonna, M. TREMs in the immune system and beyond. *Nature Rev. Immunol.* **3,** 445–453 (2003).
14. Dietrich, J., Cella, M., Seiffert, M., Buhring, H. J. & Colonna, M. Cutting edge: signal-regulatory protein β1 is a DAP12-associated activating receptor expressed in myeloid cells. *J. Immunol.* **164,** 9–12 (2000).
15. Tomasello, E. *et al.* Association of signal-regulatory proteins β with KARAP/DAP-12. *Eur. J. Immunol.* **30,** 2147–2156 (2000).
16. Kaifu, T. *et al.* Osteopetrosis and thalamic hypomyelinosis with synaptic degeneration in DAP12-deficient mice. *J. Clin. Invest.* **111,** 323–332 (2003).
17. Takayanagi, H. *et al.* T-cell-mediated regulation of osteoclastogenesis by signalling cross-talk between RANKL and IFN-γ. *Nature* **408,** 600–605 (2000).
18. Tomasello, E. *et al.* Gene structure, expression pattern, and biological activity of mouse killer cell activating receptor-associated protein (KARAP)/DAP-12. *J. Biol. Chem.* **273,** 34115–34119 (1998).
19. Takahashi, N. *et al.* Osteoblastic cells are involved in osteoclast formation. *Endocrinology* **123,** 2600–2602 (1988).
20. Takai, T., Li, M., Sylvestre, D., Clynes, R. & Ravetch, J. V. FcR γ chain deletion results in pleiotrophic effector cell defects. *Cell* **76,** 519–529 (1994).
21. Takai, T. Roles of Fc receptors in autoimmunity. *Nature Rev. Immunol.* **2,** 580–592 (2002).
22. Cerwenka, A. & Lanier, L. L. Natural killer cells, viruses and cancer. *Nature Rev. Immunol.* **1,** 41–49 (2001).
23. Aoki, K. *et al.* The tyrosine phosphatase SHP-1 is a negative regulator of osteoclastogenesis and osteoclast resorbing activity: increased resorption and osteopenia in *me*$^v$/*me*$^v$ mutant mice. *Bone* **25,** 261–267 (1999).
24. Takeshita, S. *et al.* SHIP-deficient mice are severely osteoporotic due to increased numbers of hyper-resorptive osteoclasts. *Nature Med.* **8,** 943–949 (2002).
25. Paloneva, J. *et al.* Mutations in two genes encoding different subunits of a receptor signaling complex result in an identical disease phenotype. *Am. J. Hum. Genet.* **71,** 656–662 (2002).
26. Paloneva, J. *et al.* DAP12/TREM2 deficiency results in impaired osteoclast differentiation and osteoporotic features. *J. Exp. Med.* **198,** 669–675 (2003).
27. Cella, M. *et al.* Impaired differentiation of osteoclasts in TREM-2-deficient individuals. *J. Exp. Med.* **198,** 645–651 (2003).
28. Ujike, A. *et al.* Modulation of immunoglobulin (Ig)E-mediated systemic anaphylaxis by low-affinity Fc receptors for IgG. *J. Exp. Med.* **189,** 1573–1579 (1999).
29. Takayanagi, H. *et al.* RANKL maintains bone homeostasis through c-Fos-dependent induction of *interferon-β*. *Nature* **416,** 744–749 (2002).
30. Komarova, S. V., Pilkington, M. F., Weidema, A. F., Dixon, S. J. & Sims, S. M. RANK ligand-induced elevation of cytosolic $Ca^{2+}$ accelerates nuclear translocation of nuclear factor κB in osteoclasts. *J. Biol. Chem.* **278,** 8286–8293 (2003).


**Supplementary Information** accompanies the paper on **www.nature.com/nature**.

**Acknowledgements** We thank J. V. Ravetch, H. Kubagawa and M. D. Cooper for providing materials, and M. Kaji, A. Sugahara, Y. Ito, K. Maya, A. Sato, A. Nakamura, M. Isobe, T. Yokochi, A. Izumi, T. Kohro, Y. Matsui, H. Murayama, K. Sato, M. Asagiri and I. Kawai for technical assistance and discussion. This work was supported in part by a grant for Advanced Research on Cancer from the Ministry of Education, Culture, Sports, Science, and Technology of Japan, the CREST and PRESTO programs of Japan Science and Technology Agency (JST), grants for the 21st century COE program 'Frontier Research on Molecular Destruction and Reconstruction of Tooth and Bone' and 'Center for Innovative Therapeutic Development Towards the Conquest of Signal Transduction Diseases', Grants-in-Aid for Scientific Research from JSPS and MEXT, Health Sciences Research Grants from the Ministry of Health, Labour and Welfare of Japan, grants of the Virtual Research Institute of Aging of Nippon Boehringer Ingelheim, Mochida Medical and Pharmaceutical Research Foundation and a grant from Japan Orthopaedics and Traumatology Foundation.

**Competing interests statement** The authors declare that they have no competing financial interests.

**Correspondence** and requests for materials should be addressed to H.T. (taka.cell@tmd.ac.jp) or T.T. (tostakai@idac.tohoku.ac.jp).